Available online at www.sciencedirect.com

ScienceDirect

Advances in Space Research 68 (2021) 1591–1600

ADVANCES IN SPACE RESEARCH (a COSPAR publication)

www.elsevier.com/locate/asr

Plasma-Based water purification for crewed space missions: Laboratory experimental comparisons for on-board applicability

Ryan P. Gott [*,1], Sydney D. Miller [1], Josie C. Hodges [1], Kunning G. Xu [1]

Department of Mechanical and Aerospace Engineering, University of Alabama in Huntsville, Huntsville, Alabama 35899, United States

Received 3 December 2020; received in revised form 29 March 2021; accepted 2 April 2021
Available online 20 April 2021

Abstract

Low-temperature, atmospheric pressure plasma presents a new, inexpensive, and environmentally friendly method of water purification. For long duration crewed space missions, a novel water purification system that does not rely on consumable filters and chemicals would be desirable. Plasma systems provide a viable option for these missions, but their operation and designs need to be optimized and compared to existing technology. For this application, gas and power usage are key limiting factors. In this work, water contaminated with methylene blue is purified with plasma. The rate of purification, gas flow usage, and power consumption are compared for multiple devices. A single atmospheric pressure plasma jet is compared with jet array configurations and a novel, 3D printed "plasma sheet" design that expands the size of the plasma surface area. A resource gauge parameter was developed to compare the resource usage and purification rate of each device, and this parameter showed that the plasma sheet was able to improve the rate of purification without increasing resource usage. Additionally, two types of jet arrays were designed that demonstrated the need to exceed a minimum energy and flow rate threshold to maintain effective treatment. A low cost jet was also developed that showed suitable treatment results with a two order of magnitude cost reduction. Finally, a figure of merit was discussed to compare the best performing plasma device with the urine processor assembly used on the International Space Station.

Keywords: Plasma; Water; Purification; APPJ; Spectrophotometer

1. Introduction

Clean water is a necessity of life both for crewed space exploration and here on Earth. Water reuse has become an essential element of crewed spaceflight. Water is a heavy resource used not just for drinking, cleaning, or food preparation, but also for oxygen production for respiration and potentially rocket propellant. For a long duration crewed Mars mission, it would be impractical to resupply water frequently. Currently, several kinds of water recycling methods for space are being developed or have been used on the International Space Station (ISS) and other crewed space missions. These include using iodine or silver to disinfect water (Birmele, 2011), forward osmosis (Station et al., 2018), and absorption filters (Cath et al., 2005). The Water Recovery System (WRS) on the ISS, which comprises of the Water Processor Assembly (WPA) and the Urine Processor Assembly (UPA) (Carter et al., 2018), uses a combination of distillation, an absorption bed, and a catalytic oxidation reactor. The UPA also relies on pretreatment chemicals, brine filters, and particulate filters (Volpin et al., 2020). The chemicals, catalysts, and filters are all consumable materials. Thus, a constant resupply from Earth is needed to maintain WRS operation. While this is effective for the ISS, it is not practical for deep

* Corresponding author.
E-mail addresses: ryan.gott@uah.edu (R.P. Gott), gabe.xu@uah.edu (K.G. Xu).
[1] Mechanical and Aerospace Engineering, United States.

https://doi.org/10.1016/j.asr.2021.04.001
0273-1177/

space missions where Earth resupply is difficult or impossible. The need to minimize or eliminate this dependence on resupply has become a significant focus for space agencies. A low-cost, reusable, plasma-based water recovery process that does not rely on consumable materials could alleviate some of these issues and help enable future crewed Mars missions.

Treatment of water with plasma has been of great interest in recent years. Plasma has been shown to produce many useful reactive oxygen and nitrogen species (RONs) that can cause an advanced oxidation process (AOP) to occur in water (Bo et al., 2007). The combination of the high-powered electric field, UV radiation, and reactive chemical species produced in the discharge provides the necessary ingredients for purification processes. Most importantly, plasma devices can operate continuously with the only consumable material being a feed gas. Since trash-to-gas conversion efforts have shown promising headway into providing recyclable feed gas in space (Meier et al., 2019a), this technology is a promising option for long duration crewed mission.

Plasma-based purification utilizes advanced oxidation processes (AOP) that are driven by the production of OH radicals. These radicals lead to a series of oxidizing reactions. Ozone, peroxide, water, and UV light all can play a part in the production of OH. The oxidation process mineralizes the organic materials in water to produce water, CO_2, and harmless inorganic materials. Unlike chlorine, bacteria can not develop resistance to AOP because the oxidation occurs within the microbes themselves. Plasma is a good source of the species needed for AOP. Atmospheric pressure plasmas can produce the excited species, radicals, and UV light needed to drive the process without harmful byproducts (Foster et al., 2012).

One indicator that the AOP is working in water is the decomposition of methylene blue (MB) (Aoki, Kitano and Hamaguchi, 2008; Brisset et al., 2008). MB ($C_{16}H_{18}ClN_3S$) is an organic chloride salt that has similar chemical components as urine waste, particularly when broken down. The presence of OH and other oxidative species formed by OH, such as O_3 and peroxide, cause the breakdown of chemical bonds in MB dye. Bonded molecules, such as $N(CH_3)_2$-C_6H_5 and C_6H_5-NH_2 are broken down by the decomposition reactions with the oxidative species to produce NO_3^-, C, CO_2, and water (Huang et al., 2010). Spectrophotometer measurements of solution absorbance can be used to monitor the AOP progress, as the absorbance closely represents the decomposition of the dye (Foster et al., 2013). By observing changes in the coloration of a solution after treatment, comparisons can be made between multiple devices.

Numerous designs and configurations have been studied to produce plasma for water purification (Liu et al., 2010; Foster et al., 2013; Zheng et al., 2013; Gucker, Foster and Garcia, 2015; Stratton et al., 2017; Wardenier et al., 2019). While these existing water treatment designs have shown successful purification, there are still issues with throughput and efficiency. This has prevented these devices from being used in large scale terrestrial application, but there has been success with point-of-use applications for the removal of harmful contaminants (Foster et al., 2018; Singh et al., 2020). In this work, an atmospheric pressure plasma jet (APPJ) was chosen as the main study device due to the versatility of design and demonstration of key plasma generation behaviors. Low gas temperature APPJs use high voltage pulsed dc or ac sources in combination with dielectric materials. A significant benefit of APPJ is that experiments can be conducted in-situ, meaning plants, water, and other biological materials can be treated with plasma in their natural environments. APPJ can be easily modified, operated at multiple operating conditions, and placed either inside or outside water for treatment. The adaptability of the technology makes it favorable for use in space. Our previous work studied the effects of APPJ treatment outside of water and determined the relationships between operating conditions and water treatment (Thompson, Gott and Xu, 2019). We found that higher voltages and flow rates had the most significant effect on improving treatment times.

Most plasma-based water purification systems can only treat small samples of water currently. Small jets can produce copious amounts of useful chemical species and photons but can only treat small areas. One solution to this is using arrays or jets. Plasma jet arrays often consist of multiple individual jets connected together and fed by the same power and flow system, but many designs involve developing discharge channels with broad exits or adding multiple exit orifices to a single jet (Cao, Walsh and Kong, 2009; Ma et al., 2011; Kim, Ballato and Kim, 2012; Robert et al., 2015). All designs face challenges with resource usage and physical volume, which are both important for plasma treatment. In most cases, expanding the size of the plasma surface area requires an increase in power and flow rate, which may decrease the efficiency of the process. The different plasma source designs in the literature also make direct comparisons difficult.

This work studies five different APPJ configurations for purification of MB in water and provides a unified comparison parameter. This comparison parameter helps identify a viable technology for water purification in space. A figure of merit then demonstrates the favorability of the developed technology compared to the current Urine Processing Assembly system used on the ISS. Furthermore, the key differences between each device provided insight into best practices for water treatment reactor design.

2. Materials and methods

The baseline APPJ was created using DBD technology. A stainless-steel electrode was connected to a DEI PVx 4110 pulsed module powered by a Matsusada AU-10P60 dc power supply and controlled by a DG645 digital delay generator. The electrode was housed in a quartz capillary tube that was held within a 4 mm inner diameter, 6 mm

outer diameter quartz tube. A grounded aluminium box held the setup and provided an external electrode. Helium gas flowed through the outer quartz tube where it was ionized at the electrode interface. The setup and schematic are shown in Fig. 1. Based on results of previous experiments, the jet was operated at a 9 kV voltage with a 6 kHz pulse frequency and 1 μs pulse width. The helium gas was metered at a constant flow rate of 3 standard liters per minute (slm). The operating conditions were chosen because they maximized voltage and flow rate while maintaining safe operation of the system.

A novel 3D printed version of a jet array that is contained in a single vessel, which was called the "plasma sheet" was also built and tested. The plasma sheet, shown in Fig. 2 (a) spreads the same single inlet gas flow into a two-inch-wide "sheet" of gas that is ionized. This device was operated at the same conditions as the jets (9 kV, 3 slm, 6 kHz, 1 μs).

In addition to the APPJ and plasma sheet, three other designs were studied. To measure the direct effect of surface area increases but with the same power and flow, two jets were connected in parallel to the same power and flow system. This is referred to as the "double jet" design. This effectively split the current and gas flow into each jet, thereby reducing the output of OH. A second configuration used two independent jets with separate power supplies. This is referred to as the "two jet" design. Each power supply provided 9 kV pulses. A total flow rate of 6 slm was evenly distributed between the two jets, thus matching the 3 slm, 9 kV, 6 kHz, 1 μs conditions for each jet. Lastly, with an eye towards cost-effectiveness, a low-cost pulsed dc jet was built using a high voltage high frequency transformer operating from 120 V wall power (MINMAX70). The transformer produced 7 kV, max 10 mA, ~15 μs pulse width, ~40 kHz frequency. A manual rotameter was used to provide the same the 3 slm helium flow rate. This device, shown in Fig. 2 (b) is referred to as the "LC jet" and was constructed for approximately $150.

To test the decontamination ability of each device, methylene blue dye in distilled water was used. MB was used instead of actual urine samples for health and safety as the lab does not have the appropriate biosafety level to handle human waste. MB also provides an obvious color change indicator for its removal, and its absorption has a strong peak in the visible range for the VIS-NIR spectrophotometer. While urea would be an alternative to actual human waste, the absorption spectrum of urea is primarily in the UV region, which is not accessible with the equipment.

Several solutions of the dye were made up with a concentration of 1.326e-5 M in 100 mL of water. The samples were run under the plasma jet for 15 min, 30 min, 45 min, and 60 min. After treatment, 10 mL aliquots of the samples were measured with absorption spectroscopy to determine the concentration of methylene blue dye and change in concentration of the samples. The absorbance of the 60-minute samples was checked again after the sample were sealed for seven days. This allowed for the water to return to a steady state after chemicals like peroxide were fully broken down. While peroxide wasn't directly measured in this work, the lasting changes to the water samples over time are directly related to the decomposition of the chemical (Gucker, Foster and Garcia, 2015).

The absorption of the samples was measured with a StellarNet SL1 Tungsten Halogen light source, a quartz cuvette, and an Acton SP2500 spectrometer. The spectrometer was tuned to a wavelength range of 400–800 nm to measure the 666 nm peak of methylene blue. The system actually measures the transmittance, the amount of light transmitted through the sample. The measured transmittance is then converted to absorbance by

$$A = 2 - \log\left(\frac{I_x}{I_s}\right) \quad (1)$$

Where A is absorbance, I_x is the transmittance of the test sample, and I_s is the system transmittance without

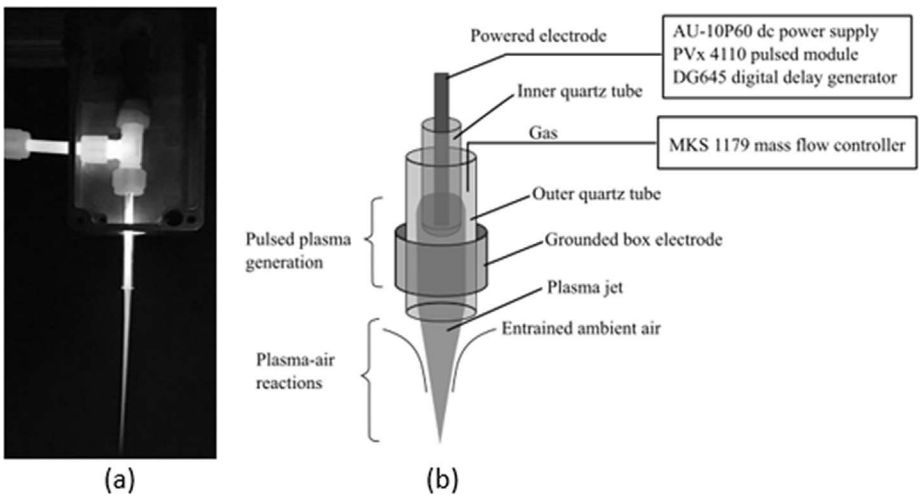

Fig. 1. A picture of the atmospheric pressure plasma jet with helium (a) and schematic of the device (b).

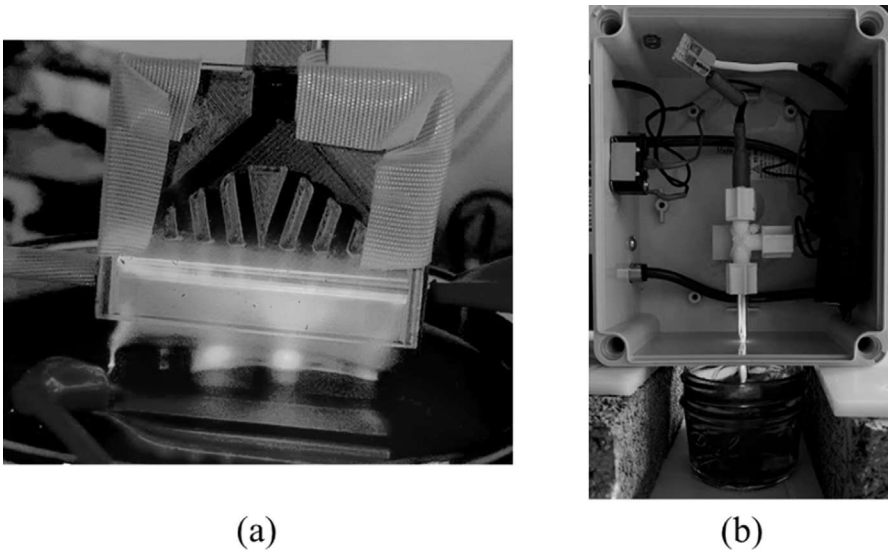

Fig. 2. The plasma sheet (a) and Low Cost (LC) Jet (b) provide two alternative plasma systems for water treatment.

any sample. Since the distilled water itself will have some absorbance, this was subtracted out by

$$A = 2 - \log\left(\frac{I_x}{I_s}\right) - \left(2 - \log\left(\frac{I_w}{I_s}\right)\right) = \log\left(\frac{I_w}{I_x}\right) \quad (2)$$

This equation provides the relative change in absorbance from the reduction of MB dye. The 666 nm absorbance value was chosen as the specific indicator of MB absorbance due to the high magnitude of absorbance at that wavelength.

The Beer-Lambert law was then used to determine the change in concentration of methylene blue in the samples. The law states

$$A = \varepsilon l c \quad (3)$$

Which can be rewritten as

$$c = \frac{A}{\varepsilon l} \quad (4)$$

Where A is absorbance, ε is the molar absorptivity (L/mol cm), l is the distance light travels through the solution (cm), and c is the concentration in mol/L. A standard quartz cuvette with sample length of 1 cm was used and the molar absorptivity was calculated from a measured calibration curve. The calibration curve was calculated by measuring the absorbance of a MB solution with a starting concentration of 3.126e-5 M and performing serial dilutions on this solution.

3. Results

Absorbance measurements gave direct insight to the amount of dye removed from water samples. A sample of the absorbance measurements for the APPJ is shown in Fig. 3. As treatment times increase, the absorbance decreases. As expected, this indicates that the concentration of MB dye also decreases. From these measurements, the percentage of dye remaining was calculated from the calibration curve. This parameter was used as the initial comparison between devices.

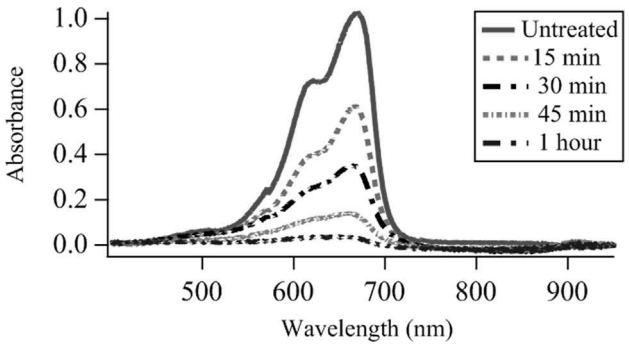

Fig. 3. The absorbance of each sample treated by the APPJ for various lengths of time. The jet operated at 9 kV, 3 slm, 1 μs, 6 kHz, and a 1 cm submersion depth.

3.1. Plasma submersion tests

In order to directly compare different devices, the operating conditions needed to be the same for all experiments. Since the voltage and flow characteristics were already determined, the remaining parameter was the location of the jet relative to the water surface. To find the optimal location, solutions of 100 mL were treated for 60 min with the exit of the single jet 1 cm above the water surface, at the water surface, and 1 cm submerged into the water. The results are shown in Fig. 4.

The submerged jet removed 92.7% of the dye compared to the 49.7% and 16.9% of the jet at the surface and 1 cm above the water, respectively. This substantial improvement led to the submersion of plasma devices in all the subsequent tests. The likely cause of this improvements is the increased amount of oxidative species that interact with

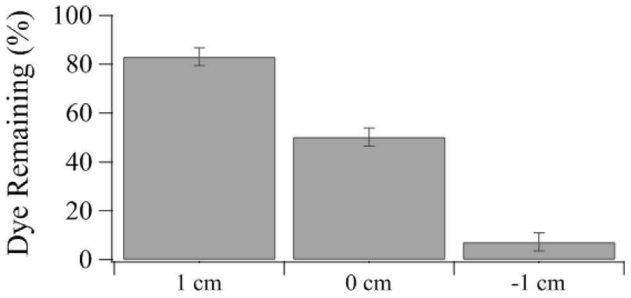

Fig. 4. The jet exit was placed at various distances in reference to the water surface. The negative distance represents a submerged jet. The samples were treated for 60 min at 9 kV, 3 slm, 6 kHz, 1 μs conditions.

the water when the distance between the electrodes and the water is minimized (Gott and Xu, 2019). Additionally, with the devices submerged, the plasma forms along the surface of the gas bubbles and the gas pocket that forms in the liquid (Foster et al., 2012). These bubbles increase the plasma-water contact area since the total surface area of the bubbles will be larger than the exit area of the jet. With the helium gas flow fully submerged, the influence of air will also be minimized. Since air has several loss mechanisms for OH and other oxidative species, the reduction in air interaction improves the rate of purification.

3.2. Comparison of jet designs

After the effects of operating conditions and submersion were determined, the different APPJ device configurations were tested and compared based on metrics of efficiency and overall removal of MB. All tests were conducted with a 9 kV voltage, 3 slm flow rate, 6 kHz frequency, 1 μs pulse width, and 1 cm submersion depth.

Each device was used to treat 100 mL water samples each with a dye concentration of 3.126e-5 M. The same treatment times of 15, 30, 45, and 60 min were used. Absorption measurements were then done for each sample. Fig. 5 shows the percent dye remaining based on the absorption measurements. The 60-minute dye concentrations are also compared in Fig. 6. Also, since it has been shown that the peroxide in the samples will continue to breakdown the dye after treatment, the samples were re-measured after 7 days. This is also shown in Fig. 6.

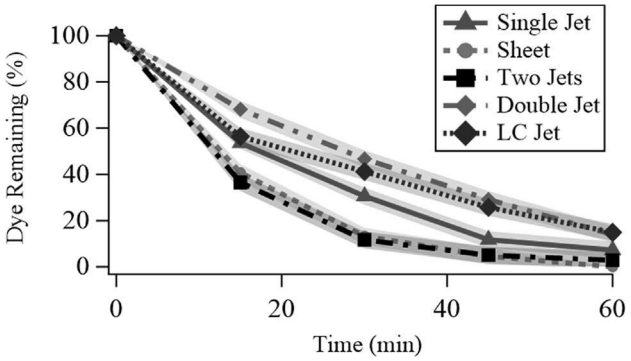

Fig. 5. A comparison of five devices treating 100 mL of water with a concentration of 3.126e-5 M. Each device was operated at a 9 kV voltage, 3 slm helium flow rate, 6 kHz frequency, and 1 μs pulse width. Error is shown as shading and is calculated from the calibration fit line error.

The double jet method performed the worst due to the drop in current and flow rate caused by splitting these resources between two jets. Each jet operated on half the current and flow of the single jet and was thus weakened, producing less overall reactive species. This is notable because it shows that higher voltages and flow rates improve the degradation of the dye at better than a linear rate. In other words, the efficiency of the degradation improves for higher voltages and flow rates. Additionally, the double jet result indicates that there is a threshold energy for each jet to be effective. This means that simply increasing the surface area by adding more jets with the same total energy input is not sufficient if each jet drops below the necessary threshold.

The two-jet method did show over twice the degradation compared to the single jet. After 60 min of treatment, 7.3% of the dye remain for the single jet versus 2.79% for the two-jet design. After seven days, the dye remaining dropped to 6.2% and 1.7%. The steady change after seven days indicates that adding a second jet does not substantially increase the peroxide production. This means that there is likely a limit to the quantity of peroxide that forms in the water sample.

The low-cost jet performed worse (14.9% remaining after 60 min) than the single jet due to the lower operating power, but the performance was comparable enough to be significant. Since the full laboratory pulsed dc system costs on the order of $20,000, the $150 system's performance is surprisingly good.

Lastly, if resource management is key, the sheet performed the best out of all designs. The sheet effectively removed all dye after 60 min of treatment. At each measured time step, the sheet removed an average of 56.5% more dye than the single jet, and the dye degradation from the sheet and two-jet design were effectively equal within the margin of error. Since the two-jet method uses twice the resources as the sheet, the sheet is better overall.

The pH, water conductivity, and temperature of all samples were also tested before and after each treatment, and the results are shown in Fig. 7.

As the plasma forms a combination of reactive species such as peroxide, the acidity of the water will increase. Additionally, the rapid bombardment of the water surface with charged species also causes an increase in conductivity over time. These effects, along with the oxidation of the water, result in an endothermic reaction that lowers the temperature of the water over time. However, the sheet design requires the electrode interface to be closer to the water surface. The electrode heats up over time due to ohmic heating, and its proximity to the water surface overcomes the loss in temperature from the reaction and results in higher water temperatures. Overall, the temperature and conductivity do not change significantly, and both are well

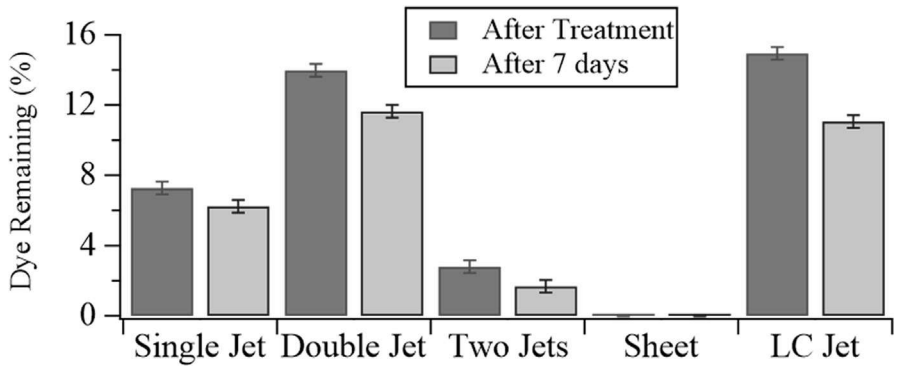

Fig. 6. The remaining dye percentage is shown for each of the devices after 60 min of treatment. The left bars in each set show the dye immediately following the treatment and shows percentages of 7.3, 14.0, 2.8, 0, and 14.9, respectively. The right bars show the dye remaining 7 days later and shows percentages of 6.2, 11.7, 1.7, 0, and 11.1, respectively.

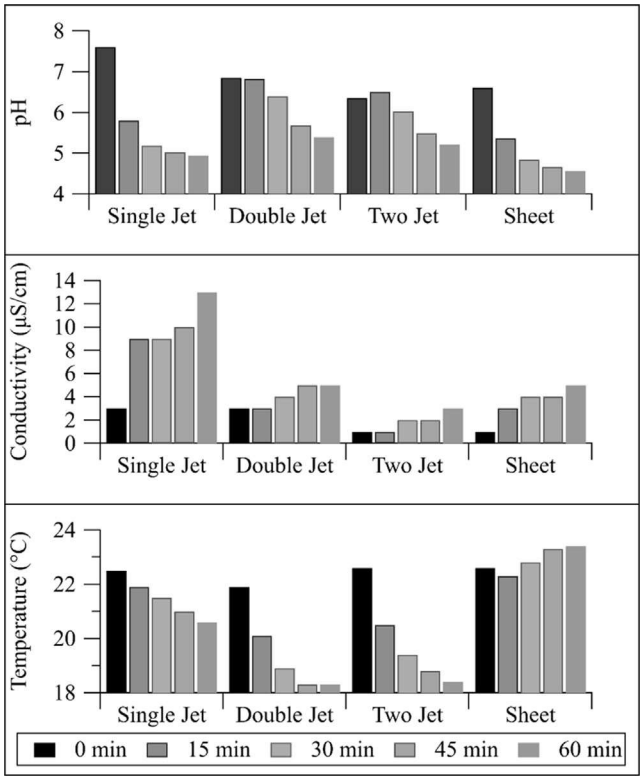

Fig. 7. The temperature, pH, and electrical conductivity of the water changed during treatment for each plasma device.

in range of potable water. However, the pH level does fall into the acidic range with a minimum value of 4.56.

4. Discussion

4.1. Design analysis

Each of the designs exhibits a unique variation that helps determine key parameters. First, the double jet shows that purely increasing plasma-water contact area does not directly lead to improved purification. However, the two jet design shows that there are improvements if the jets are operated at the same conditions. There is a threshold that both the voltage and the flow rate need to exceed for each jet to be effective. Since OH is a key driving force of the AOP, the formation of OH is a good indicator of how effective the purification rate will be. The two main OH production reactions in low temperature plasmas are electron impact dissociation and electron dissociative attachment with water, which are given by

$$H_2O + e^- \rightarrow OH + H + e^- \quad (5)$$

$$H_2O + e^- \rightarrow OH + H^- \quad (6)$$

These production mechanisms are strongly dependent on electron density. The rate constants are also strongly dependent on electron temperature (Itikawa and Mason, 2005). This is why the voltage has such a significant effect. It has been shown that both the electron temperature and electron density increase with increased input power in low temperature helium plasmas (Naveed et al., 2008). The increased electric field add energy to the electrons which increase the rate constants in (5) and (6).

Furthermore, the changes with flow rate are for similar reasons. Schlieren imaging of an APPJ at various flow rates has shown that the flow rate mainly determines the size of the gas channel (Gott and Xu, 2019). Lower flow rates thus cause the plasma to interact with a higher mole fraction of air upon exiting the tube. It has been shown that a higher helium mole fraction raises the electron temperature and electron density as well (Naveed et al., 2008; Karakas, Koklu and Laroussi, 2010).

When the plasma exits the tube, it exits a pure helium environment into a mixed gas channel. Since helium only has translational and electronic energy modes, high energy electron collisions are more likely to excite the bound electrons that lead directly to ionization. Electron collisions to produce translational energy are less likely, compared to electronic energy, due to the large mass difference between the atom and electrons. Molecular gases, which mix into the gas channel as the helium enters air, have additional rotational and vibrational internal energy modes that can absorb energy. This makes electron impact excitation of

the electronic mode less likely, thus reducing the rate of ionization. This means that air has more energy loss mechanisms and the mixing of air into the gas channel causes the plasma temperature to decrease (Ohyama, Sakamoto and Nagai, 2009). This causes a drop in electron density as well (Hemke et al., 2011). When the jet is submerged, the flow rate enlarges the gas bubble inside the water. Higher flow rates create larger bubbles, which lead to a larger surface area interaction of the plasma with water. This increases the number density of both the electrons and the water molecules in (5) and (6), which explains the significant difference between having the jet above the surface and having it submerged.

The plasma sheet avoids air losses by simply redirecting the flow. In a standard APPJ, the majority of the plasma remains localized to the powered electrode. In most jet configurations, this means the plasma is largely produced in a narrow tube, with the main exposed surface area being at the exit of the tube. The sheet changes this by having the full length of the electrode near the exit of the device. At the electrode, the gas channel is still nearly pure helium which avoids the losses in air. The increase in exposed plasma surface area without the corresponding losses in energy seen in the double jet allow for an increase in reactions (5) and (6). This in turn leads to a faster rate of purification.

4.2. Resource gauge

The plasma sheet and two-jet treatments showed faster degradation of MB dye than the single jet. However, the two-jet method used two power supplies and twice the flow resources as the other treatment methods. This makes it difficult to directly compare the two. For the sheet and jet, since the two devices operate at identical operating conditions, the improved degradation of dye is significant. In order to compare the two-jet design and any other device that uses different operating conditions, a resource usage comparison parameter is needed.

In order to calculate a useful comparison parameter, the resource and performance measures need to be determined. Input power and flow rate are the two main resources used in this work. Cost could be a third resource but does not directly affect the function of dye removal, thus is not considered here. For performance, the time required to remove the dye provides a good indication of the purification process. The decay of MB dye for each device can be modeled as an exponent decay, following the form

$$d(t) = \alpha e^{-\frac{t}{\tau}} \tag{7}$$

Here, d is the remaining dye percentage, t is the treatment time in minutes, α is the initial dye percentage, and τ is the decay time constant. An example fit for the single jet can be found in the supplemental material. The resulting equation can be used to calculate the time it takes for each device to remove 95% of the dye. Fit parameters and the time to 95% removal (t_r) for each of the devices used are shown in Table 1.

In order to calculate the input power, the current and voltage were measured for each input pulse. The current and voltage from a 9 kV, 1 μs pulse are available in the supplemental material. Integrating under the current curves and multiplying by the voltage gives the energy per pulse. By multiplying that energy by the pulse frequency of 6 kHz, the power input was determined. For the LC jet, the power input was given by the manufacturer for the power supply.

For each experiment, the t_r, input power, and flow rate should be minimized. To provide a comparison of these parameters with the purification rates, a resource gauge parameter, RG, can be calculated as follows

$$RG = \frac{1}{t_r P F} \tag{8}$$

Here, P is the input power in watts and F is the flow rate in slm. The larger the value of RG, the more efficient the system. A non-dimensional version, RG_0, can then be calculated by dividing the calculated RG by a reference value. For this work, the single jet is chosen as the reference, thus producing the values for RG_0 shown in Table 1. The calculation of RG_0 as RG/RG_{ref} indicates that values greater than 1 are desirable and values less than 1 are not.

This calculation shows that the sheet provides the best combination of treatment and resources used. The double jet uses the same amount of resources but requires a much longer treatment time than the sheet. The two-jet design provides a similar treatment time to the sheet, but doubles the resources required. For this reason, the sheet design is recommended. The LC jet is surprisingly good given its cost. It provides a proof of concept that demonstrates a low-cost plasma solution with comparable performance that shows the feasibility of using this technology around the world and in space.

Table 1
The fit and resource usage parameters are shown for each of the devices used in this work.

Device	A (%)	τ (min)	P (W)	F (slm)	t_r (min)	RG	RG_0
Single Jet	100	23.7	25	3	70.9	1.88e-4	1
Double Jet	100	36.3	25	3	108.8	1.22e-4	0.65
Two Jets	100	14.7	50	6	43.9	7.59e-5	0.40
LCJet	100	31.5	24	3	94.2	1.47e-4	0.78
Sheet	100	17.7	25	3	53.1	2.51e-4	1.34

It should also be noted that the frequency of these devices can also be reduced. The sheet, for example, can operate at a significantly lower pulse frequency of 250 Hz with only a 5% loss in MB removal compared to the 6 kHz frequency. This is significant because the reduction in frequency significantly affects the power consumption. The sheet consumes about 25 W of power when operated at 6 kHz. Reducing the frequency to 250 Hz reduces that power consumption to just 1 W. If multiple sheets were built in the same manner as the two jet design, assuming each sheet still required 3 slm of helium flow, the reduction in frequency to 250 Hz means that five sheets could be combined to achieve the same RG as the 6 kHz case. This frequency reduction effect is a significant improvement on efficiency but raises questions of what sets the minimum frequency and why higher frequencies are not useful, which will be the subject of future work.

4.3. Figure of merit

While the resource gauge is a useful comparison for plasma device designs, other purification technologies have different resource usage. Specifically, the flow rate of the gas would not be a factor for most other techniques. To demonstrate the viability of this technology for space use, an additional comparison tool is necessary. An alternative figure of merit (FOM) analysis is thus useful for these other purification techniques. For space applications, a conventional technology for comparison is the Urine Processor Assembly (UPA) that is part of the life support system on the International Space Station. The UPA is a good comparison because methylene blue dye is a chloride salt and decomposes at a similar rate to urine, which has a high percentage of chloride ions. For the UPA, the key parameters are the power usage, treatment time, and treatment volume. Thus, the FOM can be calculated as

$$FOM = \frac{V}{Pt_t} \tag{9}$$

Where V is the treated volume, P is the power, and t_t is the treatment time. The FOM assumes full decomposition of the waste/dye by any process. A comparison of the UPA to the plasma sheet, which removed all of the dye in 1 h of treatment, is presented in Table 2. The reduced frequency was used for the sheet, as that significantly reduced the power usage with comparable purification rates.

The UPA is designed to process a nominal 9 kg/day (19.8 lb/day) of wastewater consisting of urine, flush water, and a small amount of waste (Bagdigian, Cloud and Bedard, 2006; Carter, Wilson and Orozco, 2011). The UPA operates in batch mode and consumes approximately 424 W during processing and 108 W during standby. The urine is first stored in the Wastewater Storage Tank Assembly (WSTA), which has a volume of ~ 8.2 kg (18 lb), or 0.018 m^3 (18 L) if we use the density of water. Once the tank reaches ~ 70% capacity, the UPA begins a batch process cycle. Thus, the UPA processes 12.6 L (5.74 kg) per cycle, and uses 532 W of power. This equates to 1.57 cycles per day at the nominal rate, or an estimated 15.3 h per cycle. To process the same amount of liquid using the laboratory scale plasma sheet at 100 mL batches, it would take 126 cycles and consume 126 W of power. If only a single sheet was used, the total process would take 126 h. The time is easily adjustable, however, as multiple plasma sheets can be set up to run several batches at once. If five sheets were used with the power and volume divided evenly between them, the processing time is reduced to 25.2 h.

For processing the 12.6 L, the UPA has a FOM of 0.00155 L/W-hr, and using five plasma sheets together gives a FOM of 0.00397 L/W-hr. The numbers indicate that utilizing the plasma sheet alone is better with small volumes, but an array is better for large volumes. It should be noted that these plasma technologies are only at the lab scale and have room for improvement in throughput and efficiency. With access to power supplies with higher voltage capabilities, both the FOM and RG could see substantial improvements. Also, there are significant differences between a urine sample and the MB samples used here. Thus, while this FOM shows that using an array of plasma sheets may be more efficient than the current UPA, it is not a one-to-one direct comparison. Additionally, the use and cost of brine filters, water filters, and mass of the different systems are not considered in this analysis. It is anticipated that the plasma sheet array system would be significantly more cost efficient when each of these parameters is taken into account, although a full chemical analysis and a measurement of the total organic carbon in the samples would need to be completed on the sheet-treated water before it is deemed potable. Presently, however, the comparable power efficiency of the plasma sheet to the UPA in the FOM is significant because the plasma can operate without consumable filters and chemicals.

Table 2
Figure of Merit for UPA and plasma water reactor example.

Parameter	UPA	Plasma Sheet (single)	Five Plasma Sheets (match UPA volume)
Volume processed per cycle	12.6 L	0.1 L	12.6 L
Power used during cycle	424 W	1 W	126 W
Power used in standby	108 W	0 W	0 W
Cycle time	15.3 hr	1 hr	25.2 hr
FOM	**0.00155 L/W-hr**	**0.1 L/W-hr**	**0.00397 L/W-hr**

4.4. Application of technology

A key tenet of this work is the ability to utilize the technology for space use. Currently, there are numerous projects being explored at NASA's Kennedy Space Center that will implement plasma into space applications (Hintze et al., 2017; Meier et al., 2019b; Onsay, 2020). The work at NASA will conduct engineering checks such as vibrational and temperature testing and study the effects of microgravity. Those results, while not directly applied to the APPJ in this work, will nonetheless help to verify the feasibility of plasma-based purification technology for space.

While this work presents a technology in an early stage, the benefits of utilizing plasma for water treatment in space would be substantial. Improvements are needed to the current UPA system in order to have efficient water treatment on the moon and Mars. Since plasma will likely be explored for waste reduction and plant treatment, it presents a cost-effective option. Specifically, an array of plasma sheets could be easily implemented into one of these systems without significant cost. Using plasma as an alternative to the UPA would cut down on chemicals and filters and substantially reduce system mass. These changes would allow for lower launch costs and reduce the need for system maintenance.

5. Conclusion

In a short time, plasma-based water treatment has become diverse. This work presents a comparison tool for different plasma reactors. Key geometric and operational differences were also explored. A few basic designs were compared to show that higher plasma surface area and higher powers are important for water treatment. The importance of submerging this style of plasma device was also shown. Additionally, the plasma sheet provides a novel device that expands the size of the plasma without expanding resource usage. A low-cost proof of concept was also demonstrated and showed a two order-of-magnitude reduction in cost for comparable purification results.

One of the goals of this work is to be able to efficiently clean wastewater for crewed space missions. While studies of feed gas, a reduction in treatment time, and a full chemical analysis of the final treated product would likely be needed to fully implement this system on a mission, progress was made toward this goal. The increased surface area provided by the sheet and the low cost jet development both provide key efficiency improvements and show the feasibility of this technology. The sheet also compares favorably to the power efficiencies of the UPA used on the ISS. Since the plasma sheet does not utilize filters and consumable chemicals, this is a significant comparison.

To further this work, urea or actual human waste samples should be treated to provide a more direct comparison to the UPA. Air, instead of helium, could also be used as a feed gas. Optimization of plasma treatment systems also requires further study of the electrode interface where bubbles form and contain key reactive species. Finally, several plasma sheets in an array using air to treat actual human waste would be a good full-scale demonstration of this technology for use in space.

Declaration of Competing Interest

The authors declare that they have no known competing financial interests or personal relationships that could have appeared to influence the work reported in this paper.

Acknowledgements

This material is based upon work supported by the NSF EPSCoR RII-Track-1 Cooperative Agreement OIA-1655280. It is also supported by AL EPSCoR Graduate Research Scholars Program Track 14 funding.

Appendix A. Supplementary data

Supplementary data to this article can be found online at https://doi.org/10.1016/j.asr.2021.04.001.

References

Aoki, H., Kitano, K., Hamaguchi, S., 2008. Plasma generation inside externally supplied Ar bubbles in water. Plasma Sources Sci. Technol. 17 (2). https://doi.org/10.1088/0963-0252/17/2/025006.

Bagdigian, R.M., Cloud, D., Bedard, J., 2006. 'Status of the regenerative ECLSS water recovery and oxygen generation systems', in *SAE Technical Papers*. SAE International. https://doi.org/10.4271/2006-01-2057.

Birmele, M.N., 2011. Disinfection of Spacecraft Potable Water Systems by Passivation with Ionic Silver. Systems Research, 1–8. https://doi.org/10.2514/6.2011-5278.

Bo, Z. et al., 2007. Effects of oxygen and water vapor on volatile organic compounds decomposition using gliding arc gas discharge. Plasma Chem. Plasma Process. 27 (5), 546–558. https://doi.org/10.1007/s11090-007-9081-3.

Brisset, J.L. et al., 2008. Chemical Reactivity of Discharges and Temporal Post-Discharges in Plasma Treatment of Aqueous Media: Examples of Gliding Discharge Treated Solutions. Ind. Eng. Chem. Res. 47 (16), 5761–5781. https://doi.org/10.1021/ie701759y.

Cao, Z., Walsh, J.L., Kong, M.G., 2009. Atmospheric plasma jet array in parallel electric and gas flow fields for three-dimensional surface treatment. Appl. Phys. Lett. 94 (2). https://doi.org/10.1063/1.3069276 021501.

Carter, L. et al. (2018) 'Upgrades to the ISS Urine Processor Assembly', in 48th International Conference on Environmental Systems, pp. 1–7.

Carter, L., Wilson, L. L. and Orozco, N. (2011) 'Status of ISS water management and recovery', in 41st International Conference on Environmental Systems 2011, ICES 2011. American Institute of Aeronautics and Astronautics Inc. doi: 10.2514/6.2011-5223.

Cath, T.Y. et al., 2005. Membrane contactor processes for wastewater reclamation in space. J. Membr. Sci. 257 (1–2), 85–98. https://doi.org/10.1016/j.memsci.2004.08.039.

Foster, J. et al., 2012. Perspectives on the interaction of plasmas with liquid water for water purification. IEEE Trans. Plasma Sci. 40 (5 PART 1), 1311–1323. https://doi.org/10.1109/TPS.2011.2180028.

Foster, J.E. et al., 2013. A comparative study of the time-resolved decomposition of methylene blue dye under the action of a nanosecond repetitively pulsed dbd plasma jet using liquid chromatography and

spectrophotometry. IEEE Trans. Plasma Sci. 41 (3), 503–512. https://doi.org/10.1109/TPS.2013.2245426.

Foster, J.E. et al., 2018. 'Towards high throughput plasma based water purifiers: Design considerations and the pathway towards practical application', *Journal of Physics D: Applied Physics*. IOP Publishing 51 (29). https://doi.org/10.1088/1361-6463/aac816 293001.

Gott, R.P., Xu, K.G., 2019. OH Production and Jet Length of an Atmospheric-Pressure Plasma Jet for Soft and Biomaterial Treatment. IEEE Trans. Plasma Sci. 47 (11), 4988–4999. https://doi.org/10.1109/TPS.2019.2942576.

Gucker, S.N., Foster, J.E., Garcia, M.C., 2015. 'An investigation of an underwater steam plasma discharge as alternative to air plasmas for water purification', *Plasma Sources Science and Technology*. IOP Publishing 24 (5). https://doi.org/10.1088/0963-0252/24/5/055005 055005.

Hemke, T. et al., 2011. Spatially resolved simulation of a radio-frequency driven micro-atmospheric pressure plasma jet and its effluent. J. Phys. D Appl. Phys. 44 (28). https://doi.org/10.1088/0022-3727/44/28/285206.

Hintze, P. et al., 2017. Evaluation of Low-Pressure Cold Plasma for Disinfection of ISS Grown Produce and Metallic Instrumentation. 47th International Conference on Environmental Systems.

Huang, F. et al., 2010. Analysis of the degradation mechanism of methylene blue by atmospheric pressure dielectric barrier discharge plasma. Chem. Eng. J. https://doi.org/10.1016/j.cej.2010.05.041.

Itikawa, Y., Mason, N., 2005. Cross sections for electron collisions with water molecules. J. Phys. Chem. Ref. Data 34 (1), 1–22. https://doi.org/10.1063/1.1799251.

Karakas, E., Koklu, M., Laroussi, M., 2010. Correlation between helium mole fraction and plasma bullet propagation in low temperature plasma jets. J. Phys. D Appl. Phys. 43 (15). https://doi.org/10.1088/0022-3727/43/15/155202 155202.

Kim, J.Y., Ballato, J., Kim, S., 2012. Intense and Energetic Atmospheric Pressure Plasma Jet Arrays. Plasma Processes Polym. 9 (3), 253–260. https://doi.org/10.1002/ppap.201100190.

Liu, F. et al., 2010. Inactivation of bacteria in an aqueous environment by a direct-current, cold-atmospheric-pressure air plasma microjet. Plasma Processes Polym. 7 (3–4), 231–236. https://doi.org/10.1002/ppap.200900070.

Ma, J.H. et al., 2011. Microplasma jets generated by arrays of microchannels fabricated in flexible molded plastic. IEEE Trans. Plasma Sci. 39 (11 PART 1), 2700–2701. https://doi.org/10.1109/TPS.2011.2165564.

Meier, A. et al. (2019a) 'Demonstration of Plasma Assisted Waste Conversion to Gas', in 49th International Conference on Environmental Systems.

Meier, A. et al. (2019b) 'Demonstration of Plasma Assisted Waste Conversion to Gas', 49th International Conference on Environmental Systems, (July). Available at: https://www.researchgate.net/publication/334413527_Demonstration_of_Plasma_Assisted_Waste_Conversion_to_Gas (Accessed: 13 June 2020).

Naveed, M.A. et al., 2008. Langmuir probe and spectroscopic studies of RF generated helium-nitrogen mixture plasma. European Physical Journal D 47 (3), 395–402. https://doi.org/10.1140/epjd/e2008-00055-9.

Ohyama, R., Sakamoto, M., Nagai, A., 2009. Axial plasma density propagation of barrier discharge non-thermal plasma bullets in an atmospheric pressure argon gas stream. J. Phys. D Appl. Phys. 42 (10). https://doi.org/10.1088/0022-3727/42/10/105203.

Onsay, D. (2020) Researching Plant Growth in Amended Martian Regolith Simulant , Photosynthetic Rates of Plants , Seed Surface Decontamination by Plasma Methods , New Crop Development , and Porous Concrete Media, NASA Kennedy Space Center Exploration Research and Technology Programs.

Robert, E. et al., 2015. New insights on the propagation of pulsed atmospheric plasma streams: From single jet to multi jet arrays. *Phys. Plasmas*. AIP Publishing LLC 22 (12). https://doi.org/10.1063/1.4934655 122007.

Singh, R.K. et al., 2020. Removal of Poly- And Per-Fluorinated Compounds from Ion Exchange Regenerant Still Bottom Samples in a Plasma Reactor. Environ. Sci. Technol. 54 (21), 13973–13980. https://doi.org/10.1021/acs.est.0c02158.

Station, I. S. et al. (2018) International Space Station Benefits for Humanity.

Stratton, G.R. et al., 2017. Plasma-Based Water Treatment: Efficient Transformation of Perfluoroalkyl Substances in Prepared Solutions and Contaminated Groundwater. Environ. Sci. Technol. 51 (3), 1643–1648. https://doi.org/10.1021/acs.est.6b04215.

Thompson, M., Gott, R. P. and Xu, K. G. (2019) 'Efficiency of methylene blue in water purification using atmospheric plasma jet under varying conditions', in 72nd Annual Gaseous Electronics Conference. College Station, TX.

Volpin, F. et al., 2020. Urine treatment on the international space station: Current practice and novel approaches. Membranes 10 (11), 1–18. https://doi.org/10.3390/membranes10110327.

Wardenier, N. et al., 2019. 'Removal of micropollutants from water in a continuous-flow electrical discharge reactor', *Journal of Hazardous Materials*. Elsevier 362, 238–245. https://doi.org/10.1016/j.jhazmat.2018.08.095.

Zheng, C. et al., 2013. Water Disinfection by Pulsed Atmospheric Air Plasma Along Water Surface. American Institiute of Chemical Engineers Journal 59 (5).